

ABF Performance Using Covariance Matrices Derived From Spatial Spectra For Large Arrays

Joseph J. Schwarzwalder
ArgonST, Inc.
Fairfax, VA 22033
joe.schwarzwalder@argonst.com

Kathleen E. Wage
Department of Electrical and Computer Engineering
George Mason University
kwage@gmu.edu

Abstract—The covariance matrix for an array associated with a stationary space-time process is completely determined by the individual element locations, the directional responses of those elements, and the spatial spectrum of the process. Assuming the process is stationary in both time and space, there is a well-defined Fourier transform relationship between the elements of the covariance matrix and the spatial spectrum. An estimate of the covariance matrix can be determined from an estimate of the spatial spectrum. This paper compares the performance of adaptive beamformers derived from such structured covariance matrices with those based on the standard sample covariance matrix. Simulations illustrate the performance of this approach for both interference and noise only and correlated signal and interference cases.

I. INTRODUCTION

A spatially and temporally stationary space-time process can be modeled as uncorrelated plane waves arriving at the array distributed in power as a function of angle of arrival. We refer to this distribution as the spatial spectrum, $G(\omega, \phi, \theta)$, where $\{\phi, \theta\}$ are elevation and azimuth, respectively. The spatial spectrum may contain impulsive components, corresponding to discrete plane waves, and a continuous component, $G_C(\omega, \phi, \theta)$, corresponding to the smooth portion of the spectrum. For mixed spectra of this type containing K discrete plane waves with individual powers, P_k , and a continuous background component we can write

$$G(\vec{\mathbf{u}}, \omega) = \sum_{k=1}^K P_k \delta(\vec{\mathbf{u}} - \vec{\mathbf{u}}_k, \omega) + G_C(\vec{\mathbf{u}}, \omega), \quad (1)$$

where $\vec{\mathbf{u}}$ is a unit directional vector in 2 or 3 dimensions depending on the problem. For simplicity we assume a narrow band process at ω_0 , and drop the dependence on ω_0 , i.e., $G(\vec{\mathbf{u}}, \omega) \rightarrow G(\vec{\mathbf{u}})$.

For a linear array with omni-directional sensors and half-wavelength element spacing, the corresponding covariance matrix \mathbf{R} can be completely specified in terms of the individual element positions and the spatial spectrum, $G(\vec{\mathbf{u}})$ as follows. We can express the a^{th} row, b^{th} column entry in \mathbf{R} as $R(a, b)$

$$R(a, b) = S(\omega_0) \int_{\vec{\mathbf{U}}} G(\vec{\mathbf{u}}) e^{j(\omega_0/c)\vec{\mathbf{u}}^T \Delta \mathbf{p}} d\vec{\mathbf{u}}, \quad (2)$$

where $\vec{\mathbf{U}}$ contains all angles of arrival, and $\Delta \mathbf{p} = \mathbf{p}_a - \mathbf{p}_b$, the difference in position between the elements. Eq. (2) may

be a multi-dimensional integral depending on the problem. Here $S(\omega_0)$ is a scale factor that relates the normalized spatial spectrum $G(\vec{\mathbf{u}})$ to an absolute power level seen at the array. It is included for completeness, but such a scale factor does not impact adaptive beamformer weight design, therefore it can be ignored.

One could estimate the spatial spectrum, and then use Eq. (2) to estimate the corresponding covariance matrix. Given this estimate, it is possible to apply a large number of standard adaptive beamforming design algorithms. Much of the research in array processing has centered on using the sample covariance matrix, or diagonally loaded sample covariance matrix, either explicitly or implicitly, to do the same thing. Why consider this alternate approach? The reason is that the covariance matrix for this type of problem exhibits structure due to the spatial stationarity of the process and the array geometry. Processors that use structured covariance estimates have been shown to converge more quickly than processors that rely on the standard sample covariance [1], [2], making them attractive for use in non-stationary environments.

In array processing, many algorithms such as MVDR and MUSIC rely on estimates of the covariance matrix prior to estimating the spatial spectrum. As such they do not lend themselves to the use of Eq. (2) for estimating the covariance matrix. We can, however, apply classical power spectral estimation techniques to the problem without forming an estimate of the covariance matrix first. In particular, the windowed averaged periodogram is a well known technique [3]. The lesser known multitaper spectral estimation (MTSE) method of Thomson [4] accommodates mixed spectra using a harmonic analysis procedure. MTSE has the additional advantage that it is designed for situations where available data is minimal.

II. PLANE WAVES IN NOISE MODEL

Consider an N element array observing a narrowband space-time process, $x(t, \mathbf{p})$, consisting of K discrete sources with respective powers, P_k , and array manifold response vectors, \mathbf{v}_k , along with a smooth background noise component which is spatially spread across the visible region of the array. The snapshot model for this scenario can be expressed as

$$\begin{aligned} \mathbf{x}_m &= \sum_{k=1}^K \mathbf{v}_k a_k(m) + \mathbf{n}_m \\ &= \mathbf{V} \mathbf{a}_m + \mathbf{n}_m. \end{aligned} \quad (3)$$

We assume that snapshots are independent, and that the individual amplitudes, $a_k(m)$, are zero-mean complex Gaussian, $CN(0, P_k)$. The covariance matrix for this model is given as

$$\begin{aligned} \mathbf{R} &= E \{ \mathbf{x}_m \mathbf{x}_m^H \} \\ &= \mathbf{V} \mathbf{P} \mathbf{V}^H + \mathbf{R}_n, \end{aligned} \quad (4)$$

where $\mathbf{P} = E \{ \mathbf{a}_m \mathbf{a}_m^H \}$ is the covariance of the plane wave amplitudes. When the plane waves are uncorrelated, $\mathbf{P} = \text{diag}(P_1, P_2, \dots, P_K)$, otherwise the off diagonal terms represent the covariance of two of the plane waves, respectively, $P(a, b) = \sqrt{P_a P_b} \rho_{a,b}$. $\mathbf{R}_n = E \{ \mathbf{n}_m \mathbf{n}_m^H \}$ is the covariance for the background noise.

If the spatial spectrum, $G(\mathbf{u})$, were available, it could be used to estimate the covariance. Using Eq. (1) in Eq. (2)

$$\begin{aligned} R(a, b) &= S'(\omega_c) \left[\sum_{k=1}^K P_k e^{j(\omega_c/c) \mathbf{u}_k^T \mathbf{p}_a} e^{-j(\omega_c/c) \mathbf{u}_k^T \mathbf{p}_b} \right. \\ &\quad \left. + \int_{\mathbf{U}} G_C(\mathbf{u}) e^{j(\omega_c/c) \mathbf{u}^T \Delta \mathbf{P}} d\mathbf{u} \right] \\ &= S'(\omega_c) \left[\sum_{k=1}^K P_k v_k(a) v_k^*(b) \right. \\ &\quad \left. + \int_{\mathbf{U}} G_C(\mathbf{u}) e^{j(\omega_c/c) \mathbf{u}^T \Delta \mathbf{P}} d\mathbf{u} \right]. \end{aligned} \quad (5)$$

In matrix form, Eq. (5) becomes $\mathbf{R} = S'(\omega_c) [\mathbf{V} \mathbf{P} \mathbf{V}^H + \mathbf{R}_n]$, where $\mathbf{P} = \text{diag}(P_1, P_2, \dots, P_K)$. This is another way of relating that the spatial spectrum corresponds to the uncorrelated plane waves in noise model. Note that even if the snapshot data, \mathbf{x}_m , contains correlation among the plane wave components, a covariance matrix estimated using Eq. (2) will not.

III. MULTITAPER SPECTRAL ESTIMATION

Using Eq. (2) requires an estimate of the spatial spectrum, in particular one that can be determined directly from the data without first forming the covariance matrix. Classical methods such as weighted, overlapped, segment averaged (WOSA) [3] may be applied, but inherently must deal with issues of resolution, bias, and spectral leakage. Thomson's multitaper spectral estimation [4] offers a related technique that is attractive for several reasons. First, it is designed to operate with very little data, as low as a single snapshot. This makes it especially valuable for use in non-stationary environments. Second, it incorporates a technique for harmonic analysis that allows it to effectively deal with impulsive components, e.g. discrete plane waves, that cause difficulty for classical methods when encountering mixed spectra.

A. Using Multiple Tapers

Several sources describe the development of multiple taper spectral estimation, including Thomson's original paper [4],

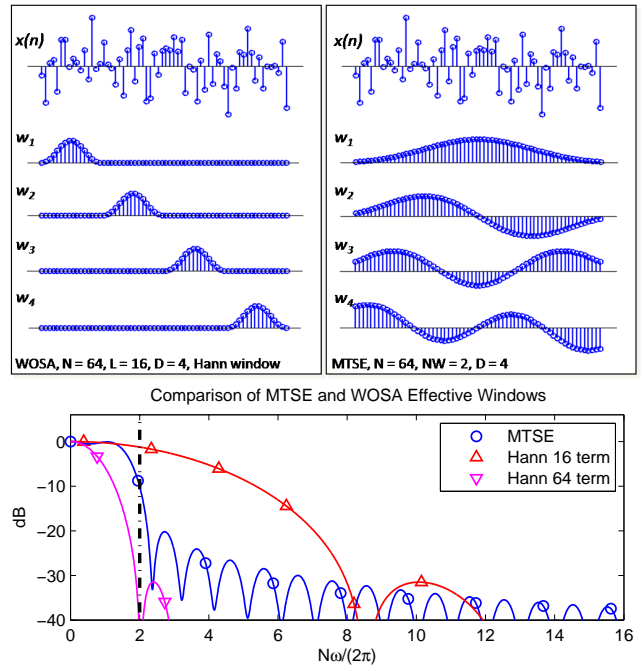


Figure 1. The general form of multi-taper spectral estimation also encompasses traditional weighted overlapped, segment averaged (WOSA) techniques. The upper left plot shows a time series divided into four non-overlapping segments using a Hann window. The upper right shows the same time series with four orthogonal windows. Both provide an improvement in estimate variance via averaging by a factor of 4, but the windows on the right use all the sample data in each estimate. Also, as seen in the lower plot, the frequency resolution is improved compared to the four Hann window approach. A single Hann window has better resolution, but does not achieve any averaging.

the text by Percival and Walden [7], and the discussion of quadratic estimators of power spectrum in [8]. Here we illustrate some of the basic differences in comparison with WOSA techniques. We will consider the framework in the context of a discrete time random process. Extension to space-time random processes follows naturally.

Given a finite observation of a stationary random process, the objective is to estimate the power contained in a particular band of frequencies, $P_\alpha = \int_\alpha S_x(f) df$. The variance of the estimate can be improved by obtaining and combining independent estimates. Thomson termed these individual power estimates eigenspectra, as their formulation comes about within the context of an eigenvalue problem for an approximate solution for P_α . The d^{th} eigenspectra is a function of the data weighted by a window (or taper), $\mathbf{w}_d(f)$, i.e.,

$$\hat{S}_d^{(mt)}(f) = |\mathbf{w}_d^H(f) \mathbf{x}|^2. \quad (6)$$

The form of the multitaper estimate then consists of a two step process. First, determine the best set of D tapers for a specified region of interest, α . For uniform sampled time series this results in solving an eigenvalue problem, with the solution being the Slepian sequences, also known as the discrete prolate spheroidal sequences (DPSS). For non-uniform sampling (or array geometry) the optimization becomes a generalized

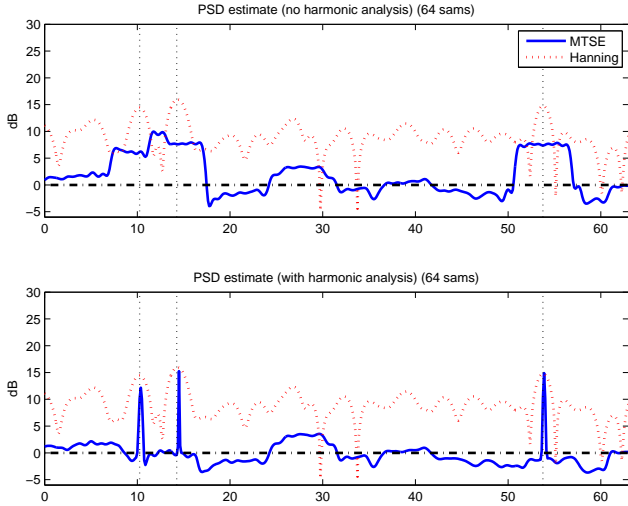


Figure 2. Harmonic analysis is the process of detecting line components and subtracting them out to estimate the residual continuous background spectrum. The upper plot shows the original MTSE spectrum for the case one 64 sample snapshot containing 3 discrete tones in noise. Similar to a classical windowed periodogram, the tone locations exhibit wide widths, with the left-most two overlapping. The lower plot shows the final MTSE spectrum post harmonic analysis (line components are added back in artificially based on estimated parameters, see [4], [18]). The resultant spectrum shows much lower variance of the background noise spectrum compared with a Hanning window periodogram.

eigenvalue problem [9]. Sets of windows determined this way differ from the effective set of multiple windows used when averaging classical non-overlapping windowed periodograms. Figure 1 illustrates the multitaper solution. The individual eigenspectra are then combined with a set of weights, $b_d(f)$, to form the final estimate

$$\hat{S}^{(mt)}(f) = \sum_{d=1}^D b_d(f) \hat{S}_d^{(mt)}(f). \quad (7)$$

The weights, $b_d(f)$, may be fixed (optimal for a white spectrum) or determined adaptively. Both approaches are discussed in [4], [7].

B. Harmonic Analysis

Harmonic analysis is the process of detecting line components within a mixed spectrum and subtracting them out in order to estimate the residual continuous background spectrum. A line component with frequency f produces a non-zero mean component in the eigenspectra at f . Defining a vector based upon the mean value of the D tapers,

$$\mathbf{W}_0(f) = \left[\sum_{n=0}^{N-1} \mathbf{w}_1(f), \sum_{n=0}^{N-1} \mathbf{w}_2(f), \dots, \sum_{n=0}^{N-1} \mathbf{w}_D(f) \right]^T, \quad (8)$$

we can define a projection matrix $\mathbf{P}_W(f)$ for the subspace spanned by $\mathbf{W}_0(f)$, and a corresponding projection matrix $\mathbf{P}_{W\perp}(f)$ for the nullspace. The presence of a line component at f can be determined for a single snapshot using the

CFAR matched subspace filter of Scharf [11], or for M multiple snapshots its extension developed by Jin [12], which effectively computes power in the line component subspace divided by power outside the subspace. Defining the inner product of the tapers and the snapshot data as

$$\mathbf{X}_{d,m}(f) = [\mathbf{w}_1(f), \mathbf{w}_2(f), \dots, \mathbf{w}_D(f)]^H \mathbf{x}_m, \quad (9)$$

the CFAR detection statistic, F defined below, can be formulated and compared to an appropriate threshold, γ , to determine the presence of a line component.

$$F = \frac{\sum_{m=1}^M \mathbf{X}_{d,m}^H \mathbf{P}_W \mathbf{X}_{d,m}}{\sum_{m=1}^M \mathbf{X}_{d,m}^H \mathbf{P}_{W\perp} \mathbf{X}_{d,m}} \underset{H_0}{\overset{H_1}{\gtrless}} \gamma \quad (10)$$

As illustrated in the example in Figure 2, harmonic analysis provides significant benefit in the case of mixed spectra, and has been shown to be effective when applied iteratively [10].

IV. SIMULATION - UNCORRELATED INTERFERERS

Consider a simulation scenario similar to the one defined by Zulch, et al. [5]. There are $K = 6$ uncorrelated jammers located at -65° , -40° , -25° , 30° , 45° , and 60° with respect to broadside. All jammers have a 50 dB jammer-to-noise ratio, specified per element and the desired signal (not present in the data) is at 0° . The arrays are linear $\lambda/2$ spacing. The noise is spatially white.

As a metric for comparison we use the normalized SINR loss, η , defined as the ratio of the SINR for the tested weights, \mathbf{w} , to the SINR of an optimal MVDR beamformer with knowledge of the true covariance matrix \mathbf{R} for desired steering vector \mathbf{s} , i.e.,

$$\eta = \frac{|\mathbf{w}^H \mathbf{s}|^2}{(\mathbf{w}^H \mathbf{R} \mathbf{w})(\mathbf{s}^H \mathbf{R}^{-1} \mathbf{s})}. \quad (11)$$

For convenience in the plots we use $\eta_{dB} = -10 \log_{10}(\eta)$, so that the positive dB value in the figures represent the loss in performance from optimal.

Two methods based on spatial spectra are considered: a Hann-windowed averaged periodogram, and Thomson's MTSE method with harmonic analysis. The adaptive beamformer weights are determined using the standard MVDR formula $\mathbf{R}_{ss}^{-1} \mathbf{s} / (\mathbf{s}^H \mathbf{R}_{ss}^{-1} \mathbf{s})$. The covariance matrix \mathbf{R}_{ss} is replaced with the estimate obtained from Eq. (2). The performance measured using MTSE to estimate the spatial spectrum is labeled the multitapered adaptive beamformer (MTABF). The Hann-windowed, averaged periodogram is labeled Hann PSD. Performance was compared to the multi-stage Wiener filter (MWF) [6] and sample matrix inversion with diagonal loading (SMI w/DL).

The MWF rank was set to the minimum of 6 (the optimal value) or the number of available snapshots. For SMI w/DL, the loading factor was found at each test point by exhaustive search for the best performance. MTSE used DPSS tapers with $NW = 2$.

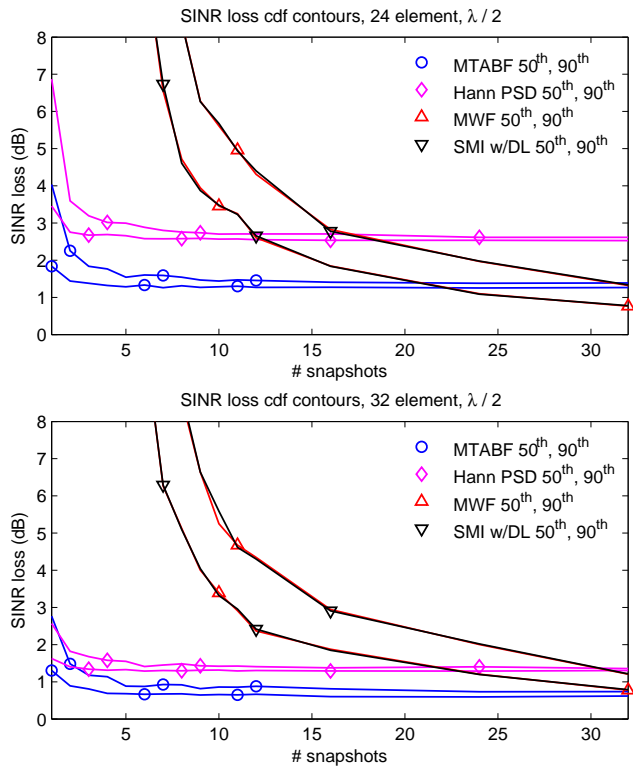


Figure 3. The plots compare the SINR loss as a function of number of snapshots for several methods of computing the ABF weights for this test case. The desired signal is at broadside and not present in the data. In the upper plot, using a 24 element array, performance for the spatial spectra techniques is better than MWF below 10 snapshots in general, with the MTSE with harmonic analysis as the best. In the lower plot, performance for a 32 element array (which has better resolving capability) shows the spatial spectra techniques improving, and MTSE with harmonic analysis still best. Note that MWF and SMI with optimal diagonal loading perform essentially identically, and that the performance is not a function of the number of elements in the array (it is driven by the number of interferers and snapshots). This is not the case for spatial spectra techniques.

While Zulch used a 16-element array, this simulation compares results for 24-element and 32-element arrays. At 16 elements the spatial spectra techniques suffer from the well known problem of spectral leakage and are unable to accurately estimate a “good” spectrum. Subsequently, performance results are poor for this number of elements. For greater number of elements, (≥ 24 in this case), the MTABF results improve substantially. Figure 3 shows the 50th (median) and 90th percentile SINR loss curves derived from 100 trials at each number of snapshots. The results indicate that very good performance can be achieved using this technique for very few snapshots for arrays of sufficient length.

V. CORRELATED SIGNAL AND INTERFERENCE

Correlated signal and interference can arise in situations of multipath between transmitter and receiver or in the event of “smart” jamming. This correlation introduces the potential for signal cancellation for some adaptive beamforming algorithms. With the both signal and interference present in the snapshot data, the MPDR beamformer attempts to minimize power

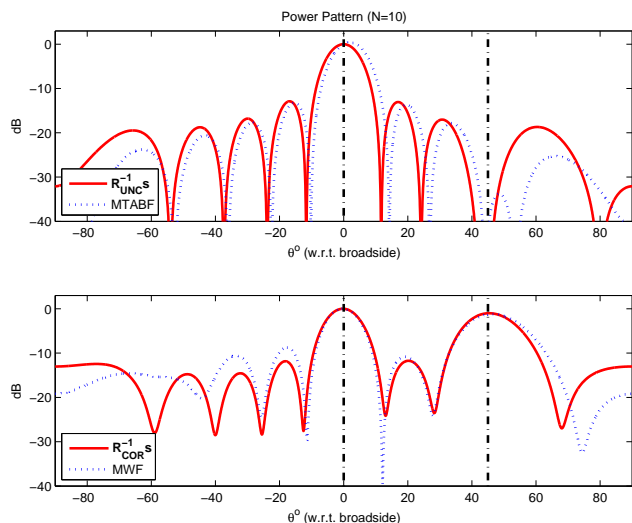


Figure 4. MVDR power pattern changes in the presence of correlated interference. This example has the desired signal at 0° and one interferer at 45° with SNR, INR = 10 dB. The upper plot has no correlation, \mathbf{R}_{UNC} , and nulls the interferer at 45° . The lower plot has $\rho = 0.90$, yielding \mathbf{R}_{COR} , and steers a beam toward 45° resulting in the signal cancellation effect. For snapshot data with $\rho = 0.90$, \mathbf{R}_{MTM} does not contain the correlation information, and $\mathbf{R}_{MTM}^{-1}\mathbf{s}$ follows $\mathbf{R}_{UNC}^{-1}\mathbf{s}$ (overlay in upper plot). For the same data, the MWF adaptive beamformer follows $\mathbf{R}_{COR}^{-1}\mathbf{s}$ and exhibits signal cancellation (overlay in lower plot).

constrained to be distortionless in the direction of the desired signal, $\mathbf{w}_{MPDR} \propto \mathbf{R}^{-1}\mathbf{s}$ [13]. MPDR allows the desired signal through, but uses the correlated interferer to destructively cancel the desired signal in the attempt to minimize output power. This is known as the signal cancellation effect. Figure 4 provides an example.

Spatial smoothing techniques have been developed to deal with correlated signal and interference at the expense of reducing the effective aperture of the array [14][15][16]. MMSE beamformers, $\mathbf{w}_{MMSE} \propto \mathbf{R}^{-1}E\{\mathbf{x}_m d_m^*\}$, use the correlation constructively to improve the output signal quality, therefore they do not suffer from signal cancellation. However, this approach is not applicable when the desired signal is unknown.

As discussed earlier, a covariance matrix estimated using Eq. (2) is based on the spatial spectrum and conveys no correlation information, even if it is present in the underlying snapshot data. This effectively mitigates the signal cancellation effect without impacting the effective array aperture.

VI. SIMULATION - SINGLE CORRELATED INTERFERER

MTABF performance was simulated for the case of a single correlated interferer. The SINR loss Eq. (11) used previously is not an appropriate metric for the correlated interferer scenario since it does not predict the impact of the signal cancellation effect. Tsai [17] analyzed this particular problem and developed closed form expressions for “effective SINR” that predict performance as a function of the individual desired signal and interferer array manifold responses, \mathbf{v}_s and \mathbf{v}_I , their

respective powers, P_s and P_I , their correlation, ρ , the spatially white noise power, σ_n^2 , and number of array elements, N .

Effective SINR, SINR_e , deliberately considers the beamformed output as consisting of three terms, $y(m) = \mathbf{w}^H \mathbf{x}_m = y_{s,m} + y_{I,m} + y_{n,m}$. $y_{s,m}$ is the desired signal, consisting of the original signal and the portion of the interference correlated with it. $y_{I,m}$ is portion of the interference that is uncorrelated. $y_{n,m}$ is the noise. The variance of these three components make up the effective SINR.

$$\text{SINR}_e = \frac{E \left\{ |y_{s,m}|^2 \right\}}{E \left\{ |y_{I,m}|^2 \right\} + E \left\{ |y_{n,m}|^2 \right\}} \quad (12)$$

SINR_e was measured via simulation for a 10 element linear array, $\lambda/2$ spacing, by varying the correlation, $|\rho|$, from 0 to 1 with uniformly random phase (following **Example 6.12.1** [13]). For each $|\rho|$, 100 trials were generated, with four snapshots per trial. The theoretical covariance was used to determine the MVDR beamformer, $\mathbf{w}_{\text{MVDR}} = \mathbf{R}^{-1} \mathbf{s} / (\mathbf{s}^H \mathbf{R}^{-1} \mathbf{s})$, and the average SINR_e measured for the output data agreed with the theoretical performance (see Figure 5). The MTABF weights were determined using the same method as earlier simulations. As seen in the Figure, MTABF performance is constant regardless of $|\rho|$ or INR, and maintains near optimal performance with MVDR in the uncorrelated case. This is accomplished without spatial smoothing therefore it does not decrease the effective aperture of the array.

VII. SUMMARY

This paper reviewed the relationship between the spatial spectrum and covariance for spatially-temporally stationary narrowband space-time processes. The spatial spectrum can be used to determine the covariance matrix, and Thomson's MTSE with harmonic analysis is particularly effective for estimating the spatial spectrum for large arrays and low snapshot support. Simulation showed adaptive beamformer performance using covariance matrices, \mathbf{R}_{ss} , computed this way have better performance with reduced numbers of snapshots than the reduced rank MWF or diagonally loaded sample matrix inversion techniques. Another useful property of this approach is its robustness to correlated interference. This is expected since \mathbf{R}_{ss} was shown to be equivalent to the uncorrelated plane waves in noise model. This is true even if there is correlation in the underlying data. Simulation of effective SINR confirmed both the known signal cancellation effect for MVDR and the robustness of MTABF in the presence of correlated interference.

ACKNOWLEDGEMENT

Work supported under Argon ST, Inc., Internal RD, R0227.08.01, and R0227.10.01.

REFERENCES

[1] S. D. Morgera and D. B. Cooper, "Structured estimation: sample size reduction for adaptive pattern classification," *IEEE Trans. Info. Theory*, vol. 23, no. 6, Nov. 1977.

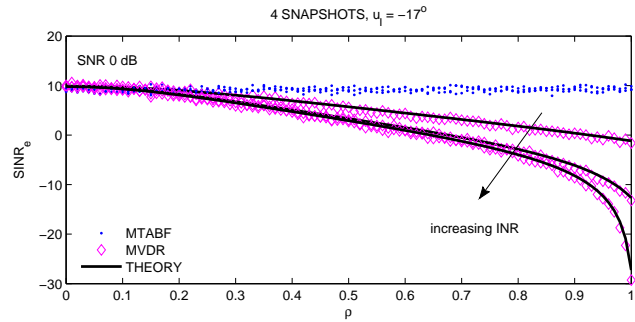


Figure 5. Effective SINR predicts the impact of signal cancellation using MVDR in the single correlated interferer case, with losses increasing with $|\rho|$. Simulation of MVDR using the theoretical covariance confirms the predicted performance. The plot shows the case of a 10 element, $\lambda/2$ linear array with 0 dB SNR and (-10, 0, 10) dB INR at -17° . The MTABF adaptive beamformer with the same data maintains $\rho = 0$ performance regardless of the true correlation, showing robustness against correlated interference.

[2] D. R. Fuhrmann, "Application of Toeplitz covariance estimation to adaptive beamforming and detection," *IEEE Trans. Signal Proc.*, vol. 39, no. 10, Oct. 1991.

[3] S. M. Kay and S. L. Marple, Jr, "Spectrum analysis - a modern perspective," *Proc. IEEE*, vol. 69, no. 11, pp. 1380-1419, Nov. 1981.

[4] D. J. Thomson, "Spectrum estimation and harmonic analysis," *Proc. IEEE*, vol. 70, no. 9, pp. 1055-1096, Sep. 1982.

[5] P. A. Zulch, J. S. Goldstein, J. R. Guerci, and I. S. Reed, "Comparison of reduced-rank signal processing techniques," in *Conf. Record of the 32nd Asilomar Conf. Signals, Syst. Comput.*, Nov. 1998, vol. 1, pp. 421-425.

[6] J. S. Goldstein, I. S. Reed, and L. L. Scharf, "A multistage representation of the Wiener filter based on orthogonal projections," *IEEE Trans. Info. Theory*, vol. 44, no. 7, pp. 2943-2959, Nov. 1998.

[7] D. B. Percival and A. T. Walden, *Spectral Analysis for Physical Applications*. New York: Cambridge University Press, 1993.

[8] M. P. Clark, L. L. Scharf, and C. T. Mullis, "Quadratic estimators of the frequency-wavenumber spectrum," in *Proc. of the Int. Conf. on Acoustics, Speech, and Signal Processing*, vol. 4, pp. 2329-2332, April 1991.

[9] T. P. Bronez, "Spectral estimation of irregularly sampled multidimensional processes by generalized prolate spheroidal sequences," *IEEE Trans. Acoustics, Speech, Signal Proc.*, vol. 36, no. 12, pp. 1862-1873, Dec. 1998.

[10] K. E. Wage, "Multitaper array processing," in *Conf. Record of the 41st Asilomar Conf. Signals, Syst. Comput.*, Nov. 2007, vol. 1, pp. 1242-1246.

[11] L. L. Scharf, *Statistical Signal Processing Detection, Estimation, and Time Series Analysis*. New York: Addison-Wesley Publishing Company, 1991.

[12] Y. Jin and B. Friedlander, "A CFAR adaptive subspace detector for second-order Gaussian signals," *IEEE Trans. on Signal Process.*, vol. 53, no. 3, pp. 871-884, March 2005.

[13] H. L. Van Trees, *Optimal Array Processing - Part IV of Detection, Estimation, and Modulation Theory*. New York: Wiley-Interscience, 2002.

[14] T.-J. Shan and T. Kailath, "Adaptive beamforming for coherent signals and interference," *IEEE Trans. Acoustics, Speech, Signal Process.*, vol. 33, no. 3, pp. 527-534, June 1985.

[15] V. U. Reddy, A. Paulraj, and T. Kailath, "Performance analysis of the optimum beamformer in the presence of correlated sources and its behavior under spatial smoothing," *IEEE Trans. Acoust. Speech, Signal Process.*, vol. 35, no. 7, pp. 927-936, July 1987.

[16] S. U. Pillai and B. H. Kwon, "Forward / backward spatial smoothing techniques for coherent signal identification," *IEEE Trans. Acoust. Speech, Signal Process.*, vol. 37, no. 1, pp. 8-15, Jan. 1989.

[17] C.-J. Tsai, J.-F. Yang, and T.-H. Shiu, "Performance analysis of beamformers using effective SINR on array parameters," *IEEE Trans. Signal Process.*, vol. 43, pp. 300-303, January 1995.

[18] S. Haykin ed., *Adaptive Radar Signal Processing*. New York: John Wiley & Sons, Inc., 2007.